

LiM 2011

Monolithical Serial Interconnects of Large CIS Solar Cells with Picosecond Laser Pulses

Gerhard Heise^{a*}, Matthias Domke^a, Jan Konrad^a, Florian Pavic^a, Matthias Schmidt^a,
Helmut Vogt^b, Andreas Heiss^b, Jörg Palm^b, Heinz P. Huber^a

^a Munich University of Applied Sciences, Lothstrasse 34, 80335 Munich, Germany

^b Avancis GmbH, Otto-Hahn-Ring 6, 81739 München, Germany

Abstract

The production of CIS thin film solar cells is still employing some mechanical steps of structuring, where thin layers have to be selectively separated in three patterns (P1 to P3) for the monolithic serial interconnection. We report on the high speed structuring of these patterns by picosecond laser ablation at 1064 nm. We demonstrate on 100x100 mm² samples, that the molybdenum back electrode can be structured with a process speed of up to 15 m/s. The ZnO front electrode film can be line separated with up to 15 m/s, the CIS absorber layer is structured with up to 4 m/s. Furthermore we extended our laser processes to 300 x 300 mm² pilot line samples which were displaying efficiencies of 13.4%.

Keywords: Thin film; solar cell; CIS; laser ablation; ultrafast laser; picosecond laser; monolithic interconnection; selective structuring

1. Introduction

Thin film solar modules can be manufactured in an economical in-line process, consuming considerably less materials than solar cells based on bulk absorbers. Especially CIS (Cu(In,Ga)(S,Se)₂) thin film solar cells are of general interest due to their high module efficiency exceeding 15 % on 300 mm² pilot line test modules [1-4]. A CIS thin film solar cell consists of the CIS p-type absorber layer sandwiched between the metallic p-contact and the transparent n-contact (see Figure 1). In order to minimize ohmic losses due to the limited conductivity of the front electrodes transparent conductive oxide (TCO) the large solar cell area is divided into smaller cells which are electrically connected in series [5].

In production patterning processes for these integrated interconnects are either based on nanosecond laser ablation [6, 7] or mechanical scribing [8, 9]. Both processes introduce damages to the thin films by mechanical forces or thermal effects. Investigations on structuring molybdenum [10, 11], CIS [10, 12] and zinc oxide (ZnO) or other transparent oxides [10, 11, 13, 14] with ultrafast lasers have shown, that pulse durations in the fs- and ps-

* Corresponding author. Tel.: +49-(0)89-1265-1646; Fax: +49 (0)89 1265 -1480.
E-mail address: gerhard.heise@hm.edu.

regime are minimizing thermal effects, but the process speed has been too slow for an industrial application [10, 12, 15, 16]. In this paper we present structuring results performed with a ps-laser on large (300 x 300 mm²) samples with industrial relevant process speeds.

2. Material and Methodes

2.1. Samples

Samples consisting of 3 mm thick float glass substrates with a size of 100 x 100 mm² are used for the feasibility demonstration and the high speed tests. Larger samples with 300 x 300 mm² are better suited to establish production processes in the pilot line and are used for efficiency tests. Sample preparation to different stages was performed at AVANCIS in the Munich R&D pilot line [3]. The P1 structuring experiments to achieve a galvanic separation of the p-contact were performed on about 0.5 μm thick molybdenum films. P2 ablation was accomplished on a stack of CIS-Mo-coated substrates. The isolating CIS layer (1- 3 μm thickness) has to be removed completely to enable a good contact of the molybdenum layer to the ZnO layer being deposited in a later process step. The P3 separation of the n-contact by mechanical scribing removes the complete combined ZnO/CIS layer on top of the Mo. With ps laser ablation it is advantageous to ablate only the highly conductive transparent ZnO layer (1 -2 μm) on top of the CIS because a higher processing speed can be achieved and a lower thermal impact is inflicted upon the remaining layers.

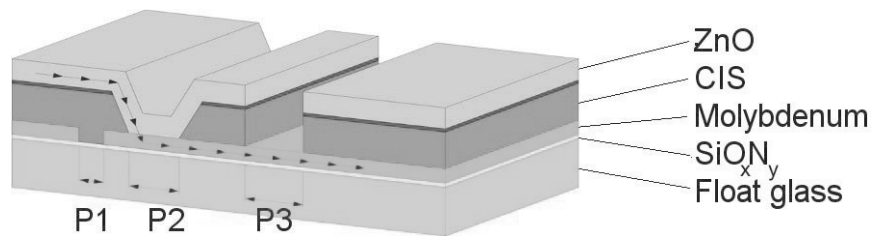


Figure 1. Schematic cross-section of the serial interconnect region of a CIS thin film solar cell. The glass substrate is carrying a below 1 μm thick molybdenum-layer as p-contact followed by 1-3 μm thick CIS absorber layer covered by a 1 – 2 μm transparent ZnO-layer as n-contact. The regions labeled with P1, P2 and P3 are indicating the structuring patterns for the monolithic serial connection. The chain of arrows is displaying the path of the electron flow.

2.2. Laser processing system

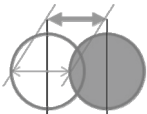
The applied laser source is a High Q Laser picoREGEN UC-30000 (1064 nm) with a pulse duration of about 10 ps at a repetition rate up to 950 kHz and a maximum power of 30 W. An optical pulse picker allows adjusting the repetition rate of the system without affecting the pulse energy. The laser is integrated in an Innolas Systems ILS 500X laser processing system equipped with two orthogonal linear stages for sample positioning and devices for beam delivery. A vertical linear stage is carrying the focusing system with a galvanometric scanner and the vision system for focus adjustment with respect to the sample and the recovery of alignment marks and previously recorded patterns, respectively. Exact focusing is important, especially because the distance of focus is different for processes with laser incidences directly upon the coating (P2, P3) compared to irradiation through the glass carrier for P1 lift off processes.

The galvanometric scanner is used to move the laser beam over the substrate with process speeds up to 15 m/s. The field of view of the scanner system is limited to 160 x 160 mm², which is sufficient only for the 100 mm samples. To scribe longer lines the 300 mm samples are moved with a speed up to 1 m/s using the linear stages of the system while the laser beam remains at rest.

The optical power of the laser is measured with an optical power meter integrated in the working chamber. The beam waist was measured with a Primes Micro Spot Monitor. A beam waist $2w$ of typically 40 μm (diameter at $1/e^2$ -intensity) at the sample was achieved forming the beam with an optical telescope and a 250 mm focusing lens. From these measurements the fluence of the laser pulse is calculated.

To scribe continuous lines with a pulsed laser, adjacent ablated spots must overlap. Hence, the scribing speed v depends on laser spot size $2w$, the repetition rate f and the overlap factor OL as given by (1). Assuming a spot size of 50 μm , a repetition rate of 1 MHz and an overlap factor of 0.5, a maximum speed of 25 m/s is achievable.

The overlap factor is defined here with respect to the lasers spot diameter. The overlap calculated with the ablated spots diameter as seen in the figures below may differ.

$$\Delta s = 2w \cdot (1 - OL)$$


$$v = \frac{\Delta s}{\Delta t} = 2w \cdot (1 - OL) \cdot f \quad (1)$$

3. Results

3.1. P1 patterning of molybdenum

The galvanic separation of molybdenum is achieved by irradiating the metal layer from the glass side; see Figure 2, right side. This lift-off process is based on direct induced laser ablation and utilizes the lasers energy very efficiently, allowing a high speed structuring process[17]. Trenches have been scribed with repetition rates between 10 kHz and 950 kHz. The ablation threshold remained nearly independent of repetition rate. Thus, an interaction between adjacent spots can be neglected and line scribing behaves like a single pulse.

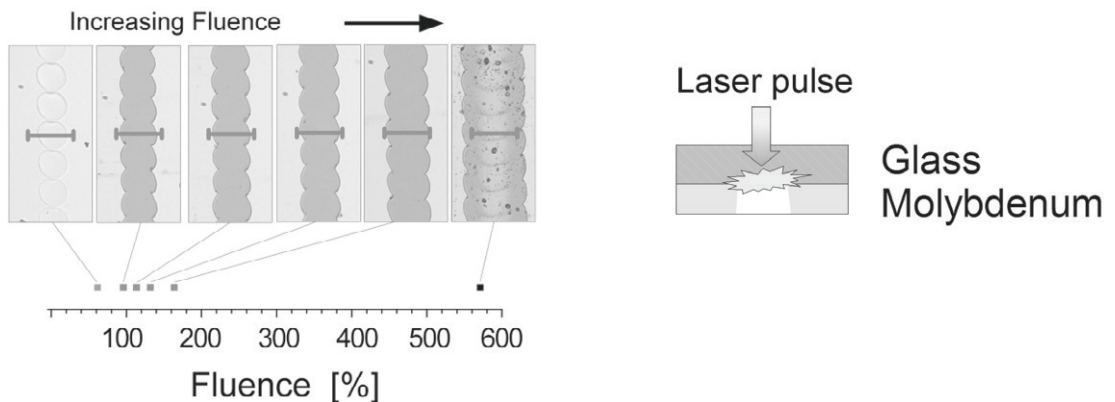


Figure 2. P1 pattern in molybdenum scribed from the glass side (schematic sketch to the right) with increasing fluence at a scribing speed of 15 m/s, microscopic images with front and back side illumination. The light blue region corresponds to the exposed buffer layer. The length of the red bars corresponds to 30 μm . The red squares mark the range of fluences where high quality trenches are possible.

We achieved processing speeds up to 15 m/s, limited both, by the speed of our scanner system and by the repetition rate of the laser system, see (1). The limits of the process, see figures at low fluence are determined by the requirement to achieve full galvanic separation between every cell. On the high fluence side, the applied laser fluence must not exceed the damage thresholds of neither the SiO_xN_y buffer layer nor the glass substrate below the metal layer. In Figure 2, left side we show optical microscope images of trenches written with increasing fluence and a repetition rate of 950 kHz. The two outermost rows demonstrate these limits. For the leftmost row, the fluence was too low to punch out the molybdenum. Profiler measurements reveal a bubble formation in the metal film with a height of ca. $0.5 \mu\text{m}$, see Figure 3, left. In the rightmost row, damage of the buffer layer below the molybdenum electrode is visible with backlight illumination.

Details of the failure mechanisms are given in Figure 3. They show confocal images and profiles of bulges at too low fluences and damage at too high fluences.

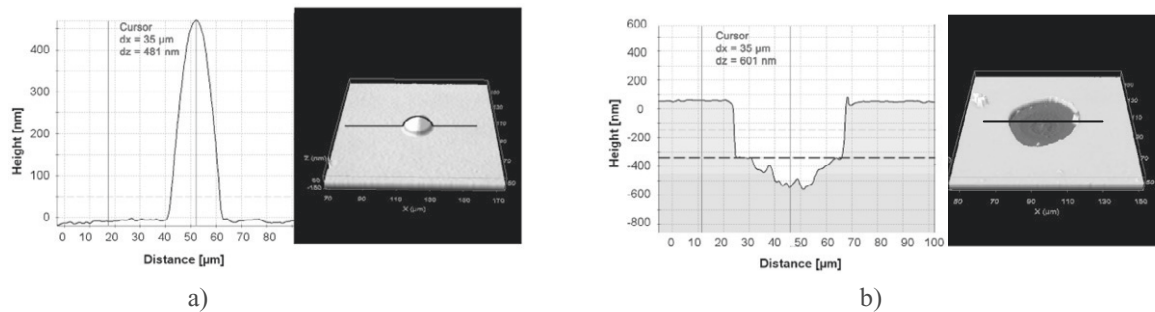


Figure 3. Confocal image profiles demonstrating the P1 process limits for single spot ablation with respect to laser fluence. The left and right graphs correspond to the leftmost and rightmost columns of Figure 2. The black lines in the 3D view indicate the position of the profiles.

a): Fluence too low → molybdenum forms bulges.

b): Fluence too high → buffer layer destroyed. (The dashed line in the profile indicates the interface molybdenum layer to buffer layer (buffer in green, glass substrate in red))

3.2. P2 patterning of CIS

The P2 layer has to enable a highly conductive contact between the n-conducting ZnO and the molybdenum p-contact. Hence the molybdenum at the bottom of the grooves must not be damaged, and there should not remain any residues in the grooves. The composition of the CIS used here is designed to harvest also the near infrared part of the solar spectrum so that it is highly absorptive for light with a wavelength of 1064 nm [18]. Other groups reported that their CIS is nearly transparent at that wavelength giving rise to a completely different ablation behavior [19].

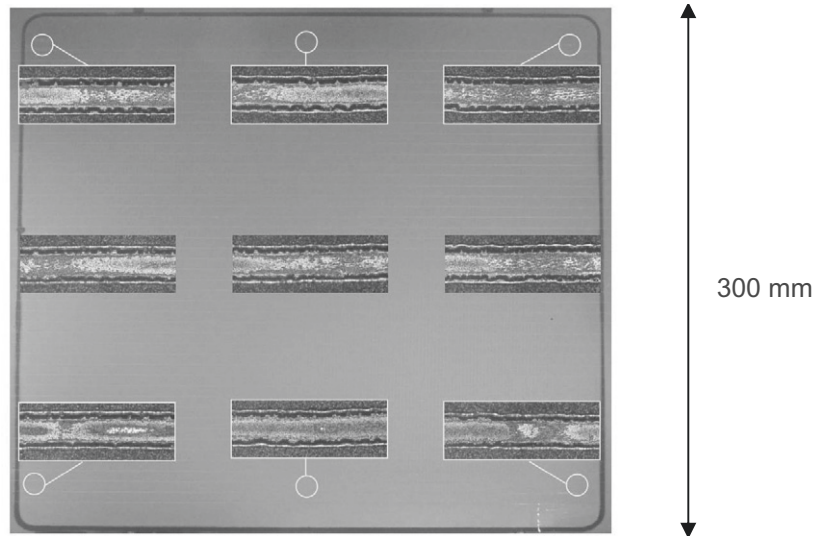


Figure 4. P2 trenches in 300 x 300 mm² sample, photograph of the complete pane. The microscopic image insets are taken at the positions on the sample marked with the yellow circles. The width of the displayed trenches is about 20 μm

In our case a single pulse ablates only typically 100 nm of the CIS if fluence is low enough not to damage the molybdenum below it. Therefore, the P2 trenches are scribed with fluences below 1 J/cm² but with a high pulse overlap of more than 90 %. According to (1) this is reducing the process speed considerably.

The P2 trenches have to be aligned with the previously fabricated P1 grooves. Their position is measured using the vision system. The trenches in the 300 mm sample shown in Figure 4 have been written with 1 m/s at 950 kHz. To enable a high speed processing of this large sample each quarter of the sample was patterned using the scanner. When one quarter was completed, the sample was repositioned accordingly with the motorized linear stages in a step and repeat manner. Figure 5 shows a confocal image profile of the P2 trench. The bulging at the sidewalls is probably due to heat accumulation caused by the high pulse overlap. However they do not affect the overgrown ZnO., and we achieved aperture solar module efficiency of up to 13.4 % applying this laser P2 process on 30 cm x 30 cm substrates.

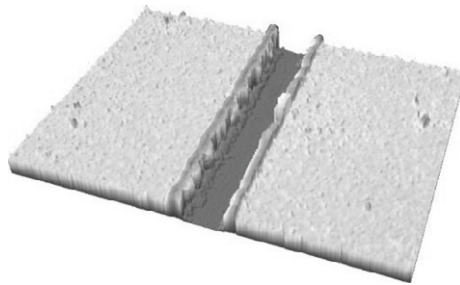


Figure 5. Confocal image profile of a P2 trench. The width of the trench is about 30 μm, its depth less than 3 μm.

3.3. P3 patterning of zinc oxide

Figure 6 displays P3 trenches that have been written with the same laser equipment. Only the ZnO has been removed. Like P1 from the glass side, this is also an induced laser ablation process with low pulse overlap and no interaction between the single pulses [20]. In contrary to P1 here the underlying CIS is the absorbing partner and the ZnO is the transparent partner. The laser ablation of the ZnO is indirect induced by the underlying CIS. The confocal image profiles show from left to right patterns scribed with the ablation speed increasing from 10 to 14 m/s. In this case, the single pulse fluence and the repetition rate were kept constant, but the pulse overlap was decreased from 50 to 30 %.

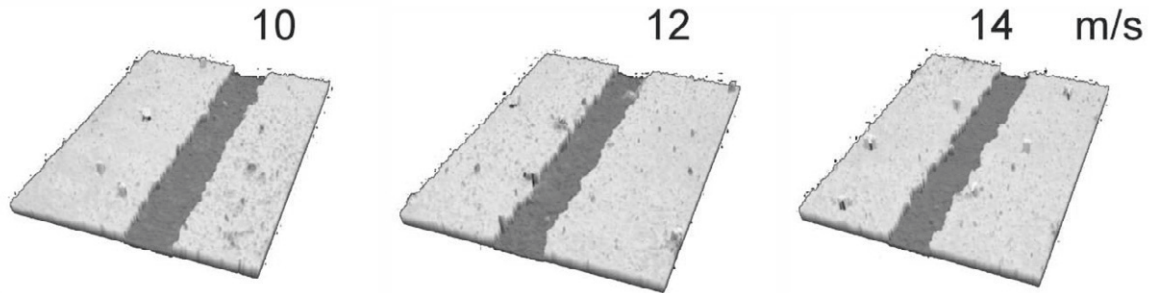


Figure 6. Confocal image profiles of P3 (only zinc oxide removed) trenches scribed with decreasing pulse overlap and a speed from 10 m/s (left) to 14 m/s (right).

4. Discussion

When a process is transferred from smaller (100 x 100 mm²) to larger substrates (300 x 300 mm²), several aspects are changing.

- **Speed:** For galvanometric scanners with a given optical resolution, the field of view is limited; however its speed exceeds that of mechanical stages by far. To take full advantage of their high speed, we tried a step and repeat procedure. But even with careful alignment, one has to take care for some error giving rise to either interrupted lines or a double exposure. Interruptions are critical for P1 and P3 as they result in remaining short cuts. In the case of P2, the current may easily flow around a not too large interruption. Double exposure is not critical for P1, but it might damage the molybdenum layer in P2 and introduce additional shunts in P3. Best aperture module efficiency up to now was 13.4 % for samples with P2 grooves generated in this step and repeat procedure with a double exposed region of about 100 μm. To avoid the risk of short cuts, the P1 and P3 trenches of 300 mm² wafers have been written with a fixed laser and a mechanically moved sample at speeds in the range of 300 mm/s.
- **Reliability:** The requirements on the reliability, stability and robustness of the process increases with the size of the samples. On a single sample of 100 mm², the total length of each pattern is 1.2 m. If e.g. a short cut happened on average every 10 m, every 8th wafer is affected. On 300 mm² samples with a total length of each pattern of 13.5 m almost every sample will be affected! The acceptable error rate is strongly dependent on sample area, i.e. it decreases nearly one order of magnitude changing from 10 cm x 10 cm samples to 30 cm x 30 cm.
- **Positioning accuracy:** The region of the monolithic interconnects should be as small as possible. Therefore the patterns P1 to P3 should be as close as possible. Given a certain safety distance between the lines, the 300 mm

samples require a 3 times better accuracy for the angular alignment than the 100 mm wafers to guarantee the patterns parallelism.

5. Conclusion

The high speed patterning for the monolithical serial interconnection of CIS thin film solar cells with picosecond laser pulses has been demonstrated successfully. We achieved speeds up to 15 m/s for the P1 molybdenum removal at full galvanic separation and for the P3 ablation of ZnO on CIS on 100 mm x 100 mm samples. These picosecond laser ablation processes appear to be essentially a single pulse process (direct and indirect induced laser ablation) and the process speed is limited by the equipment, namely the scanner speed and the repetition rate of the laser source. Scribing wafers of 300 mm² or larger, the speed is limited by the speed of the applied mechanical stages. A transfer of the realized high scribing speeds to larger samples would require a different machine concept. Scribing of P2 patterns is a multi pulse process and based on direct laser ablation, which reduces the speed according to the higher overlap factor. 300 mm samples have been patterned with P2 scribing speeds of 1 m/s using a step and repeat method, with this technique we achieved solar aperture efficiency of up to 13.4% for modules with laser P2.

Acknowledgements

This work was funded by the German Federal Ministry for the Environment, Nature Conservation and Nuclear Safety within the project “SECIS”. We thank Helmut Herberg and Michael Kaiser from Munich University of applied Sciences for the help with confocal image profiling.

References

- [1] Avancis GmbH, Press Release 2. 1. 2010
- [2] M.A. Green, K. Emery, Y. Hishikawa, W. Warta, *Prog Photovoltaics Res Appl* 18/5 (2010) 346.
- [3] V. Probst, J. Palm, S. Visbeck, T. Niesen, R. Tölle, A. Lerchenberger, et al., *Sol Energ Mater Sol Cells* 90/18-19 (2006) 3115.
- [4] I. Repins, M.A. Contreras, B. Egaas, C. DeHart, J. Scharf, C.L. Perkins, et al., *Prog Photovoltaics Res Appl* 16/3 (2008) 235.
- [5] B. Dimmler, M. Powalla, R. Schaeffler, *Conference Record of the IEEE Photovoltaic Specialists Conference*, Lake Buena Vista, FL, 2005, p. 189.
- [6] A.D. Compaan, I. Matulionis, S. Nakade, *Opt Lasers Eng* 34/1 (2000) 15.
- [7] C. Molpeceres, S. Lauzurica, J.L. Ocana, J.J. Gandia, L. Urbina, J. Carabe, *J Micromech Microengineering* 15/6 (2005) 1271.
- [8] B. Dimmler, H.W. Schock, *Prog Photovoltaics Res Appl* 4/6 (1996) 425.
- [9] V. Probst, F. Karg, J. Rimmasch, W. Riedl, W. Stetter, H. Harms, et al., in: G. D., C. A., S. H.W., E. C., P. T.M., W. T. (Eds.), *Materials Research Society Symposium - Proceedings*, Materials Research Society, San Francisco, CA, USA, 1996, p. 165.
- [10] J. Hermann, M. Benfarah, S. Bruneau, E. Axente, G. Coustillier, T. Itina, et al., *J Phys D* 39/3 (2006) 453.
- [11] H. Huber, S. Zoppel, J. Zehetner, R. Merz, M. Lederer, W. Seitz, et al., *LAMP 2006, International Congress on Laser Advanced Materials Processing*, Kyoto, 2006.
- [12] D. Ruthe, K. Zimmer, T. Hoeche, *Appl Surf Sci* 247/1-4 (2005) 447.
- [13] J. Hermann, M. Benfarah, G. Coustillier, S. Bruneau, E. Axente, J.-F. Guillemoles, et al., *Appl Surf Sci* 252/13 SPEC. ISS. (2006) 4814.
- [14] G. Raciukaitis, M. Brikas, M. Gedvilas, T. Rakickas, *Appl Surf Sci* 253/15 (2007) 6570.
- [15] S. Zoppel, H. Huber, G.A. Reider, *Applied Physics A: Materials Science & Processing* 89/1 (2007) 161.
- [16] H.P. Huber, F. Herrnberger, S. Kery, S. Zoppel, *Proceedings of SPIE*, San Jose, CA, 2008.
- [17] G. Heise, M. Englmaier, C. Hellwig, T. Kuznicki, S. Sarrach, H. Huber, *Appl Phys A* 102/1 (2011) 173.
- [18] F.H. Karg, *FVS Themen/* (2000) 145.
- [19] F.J. Pern, L. Mansfield, S. Glynn, B. To, C. DeHart, S. Nikumb, et al., *35th IEEE Photovoltaic Specialists Conference*, Honolulu, 2010.
- [20] G. Heise, M. Domke, M. Dickmann, A. Heiss, T. Kuznicki, I. Richter, et al., *accepted by Applied Physics A: Materials Science & Processing* (2011).